phys. stat. sol. (a) **188**, No. 2, 889–893 (2001)

Influence of Doping Profiles on p-type AlGaN/GaN Superlattices

E. Waldron[1]), J. Graff, and E. Schubert

Department of Physics and Department of Electrical and Computer Engineering, Boston University, 8 Saint Mary's Street, Boston, Massachusetts 02215, USA

(Received June 21, 2001; accepted July 12, 2001)

Subject classification: 73.21.Cd; S7.14

Transport properties of modulation-, shifted-modulation-, and uniformly doped $Al_{0.20}Ga_{0.80}N$/GaN superlattices are reported. The modulation-doped sample is doped only in the AlGaN barriers. The shifted-modulation-doped sample has its dopants shifted by one-quarter period. Measurements reveal a strong improvement in mobility and resistivity for the modulation-doped and shifted-modulation-doped structures versus the uniformly doped structure. The modulation-doped sample has a mobility of 9.2 and 36 cm^2/Vs at 300 and 90 K, respectively, and a very low resistivity of 0.20 and 0.068 Ωcm at 300 and 90 K, respectively. Capacitance–voltage profiling shows multiple two-dimensional hole gases. The results are consistent with a reduction of neutral impurity scattering for modulation-doped structures as compared to uniformly doped structures.

Introduction Mg acceptors in GaN and $Al_xGa_{1-x}N$ have an activation energy of 150–250 meV [1–3], much larger than kT at 300 K, resulting in low activation and therefore low conductivity in p-type GaN, degrading the performance of LEDs, lasers, and heterojunction bipolar transistors. The strong temperature dependence of the transport properties is problematic for device operation at high as well as low temperatures where carrier freeze-out occurs. The p-type $Al_xGa_{1-x}N$/GaN doped superlattices have been demonstrated to have higher acceptor activation [4–7] resulting in low resistivity. This can be further improved by minimizing ionized and neutral impurity scattering mechanisms through modulation doping.

In this work, the effect of modulation doping in $Al_{0.20}Ga_{0.80}N$/GaN superlattices is investigated using Hall-effect and C–V profiling techniques. We show the modulation-doped (MD) and shifted-modulation-doped (SMD) samples to have superior electrical properties compared to uniformly doped (UD) samples, especially at low temperatures. Furthermore, C–V profiles are presented that show the multiple two-dimensional hole gases (2DHGs) of the superlattice structure.

Sample Descriptions and Experimental Techniques The Mg-doped gallium-faced superlattices (SLs) were grown by molecular-beam epitaxy (MBE) on c-plane sapphire substrates. All doped regions have a Mg concentration of $N_{Mg} \approx 10^{19}$ cm^{-3} and all samples have an equal barrier and well width of 100 Å. The MD, SMD, and UD samples have 20, 20, and 15 periods, respectively. Only the barrier layers of the MD sample are doped whereas the well layers are undoped. The SMD sample is identical to the MD sample except that the SMD dopants are shifted one-quarter period away from the epilayer surface. The UD sample has both the $Al_{0.20}Ga_{0.80}N$

[1]) Corresponding author; Phone: 001-617-353-1912; Fax: 001-617-353-0101; e-mail: ewaldron@bu.edu

© WILEY-VCH Verlag Berlin GmbH, 13086 Berlin, 2001 0031-8965/01/18811-0889 $ 17.50+.50/0

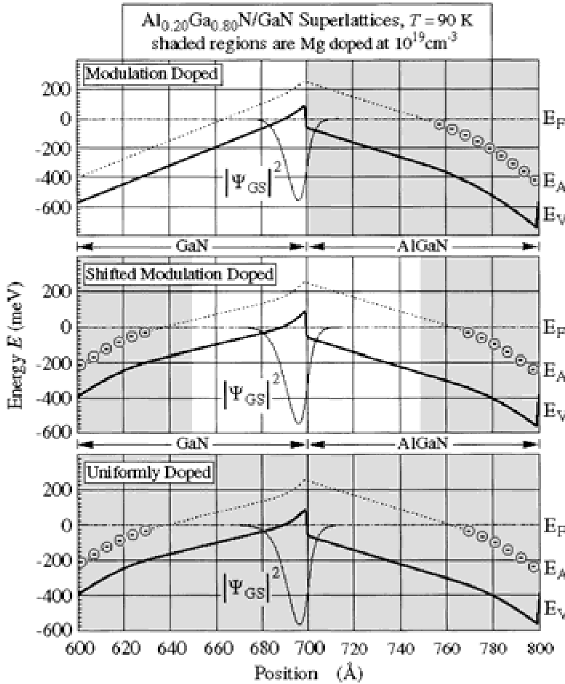

Fig. 1. Self-consistent valence band diagrams of a modulation-doped superlattice, a shifted-modulation-doped superlattice and a uniformly doped superlattice. The three ground state hole energies are $E_0 - E_F = -5.9$, -1.7, and -1.7 meV, respectively. Ψ^2 is the self-consistently solved ground-state wavefunction. It is the only occupied subband at 90 K. The epilayer surface is on the left side of the figure

barrier and GaN well layers doped. The doping profiles of all samples are shown in Fig. 1.

The variable temperature Hall-effect measurements are performed from 90 to 390 K in 10 K increments using the van der Pauw geometry. Pd/Au p-type ohmic contacts are deposited using electron beam evaporation. A CRYO Industries cryostat is used and the magnetic field is 0.5 T. The $C-V$ profile uses a mercury probe in conjunction with an HP 4194A Impedance/Gain-Phase Analyzer using a voltage sweep from 0 to 6 V. A low measurement frequency of 5 kHz is required to reduce the effects of parasitic series resistance.

Theory SL structures use materials with different bandgaps and, in the case of the III-nitrides, large internal polarization fields [8–10]. A bound surface charge results when $\mathbf{P} \cdot \hat{\mathbf{n}} \neq 0$, where $\mathbf{P}$ is the polarization at the surface and $\hat{\mathbf{n}}$ is the surface normal. A bound interface charge results when $\nabla \cdot \mathbf{P} \neq 0$, where $\mathbf{P}$ is the internal polarization. These charges occur at each interface within the superlattice. The result of the bound polarization charges and modulated band gap is a tilting of the valence band within the barriers and wells, as displayed in Fig. 1. Free holes are created when the acceptor level is near or below the Fermi level. Holes accumulate along those SL interfaces where the valence band is near the Fermi level, giving origin to a 2DHG.

The band diagrams in Fig. 1 are calculated self-consistently using a 1D Schrödinger-Poisson solver [11]. An $Al_xGa_{1-x}N$ hole mass [9] of $(1.76 + 1.77\,x)\,m_{e,\,z}$, valence band discontinuity of $0.3\,E_g$, and energy gap $E_g(x) = (3.425 + 2.71\,x)$ eV is used, x being the aluminum concentration. The hole probability density is shown in Fig. 1 for each type of SL. At 90 K, only the ground states are occupied. The Mg ionization energy in

Table 1
Hall-effect data of doped $Al_{0.20}Ga_{0.80}N$/GaN superlattices

	MD	SMD	UD
300 K mobility (cm^2/Vs)	8.9	5.6	3.0
90 K mobility (cm^2/Vs)	36	18	2.0
300 K resistivity (Ωcm)	0.21	0.66	0.81
90 K resistivity (Ωcm)	0.068	0.21	0.84
300 K carrier concentration (10^{18} cm^{-3})	3.4	1.7	2.6
90 K carrier concentration (10^{18} cm^{-3})	2.5	1.6	3.7
activation energy (meV), T = 250 – 390 K	16	13	30

AlGaN is not known precisely. However, recent results have shown that the ionization energy of Mg acceptors in $Al_xGa_{1-x}N$ increases from ≈170 to 360 meV for x = 0 to 0.27, respectively [12, 13]. We therefore use a simple Vegard-like relationship and put the acceptor level, E_A, at (170 + 704x) meV above the valence band.

Experimental Results Values of the hole mobility at selected temperatures are given in Table 1. Variable temperature data, not shown here, reveal the mobility of the MD and SMD SLs increases monotonically with decreasing temperature, indicative of the reduced influence, compared to the UD SL, of ionized impurity scattering and the presence of a 2DHG. All samples show a reduction of mobility at higher temperatures due to a combination of phonon and piezoelectric scattering [14]. Because the GaN family is strongly polar and AlGaN/GaN superlattices contain strong polarization fields [15], polar optical phonon scattering is expected to be the dominant scattering mechanism at temperatures above ≈150 K.

The reduction of neutral impurity scattering in the MD and SMD SL is expected since their 2DHG channels contain no intentional Mg dopants. The neutral dopants in the UD SL channels cause a sharp decrease in mobility at low temperatures $\propto T^{3/2}$. Note that the MD SL exhibits a clearly higher mobility and lower resistivity than the SMD SL. These differences are not yet well understood and are subject to further investigations.

The resistivity of the SL samples vs. temperature is shown in Fig. 2. There is an improvement for the MD and SMD SL compared to the UD SL. At 300 K, the resistivity is 0.21 Ωcm for the MD SL. The lowest resistivity of the MD SL occurs at 90 K and is 0.068 Ωcm, the lowest reported resistivity for p-type GaN and $Al_xGa_{1-x}N$ material. Table 1 contains selected resistivity values. Particularly noteworthy is the resistivity of the MD and SMD SL, which is lower than the UD SL at all temperatures and decreases monotoni-

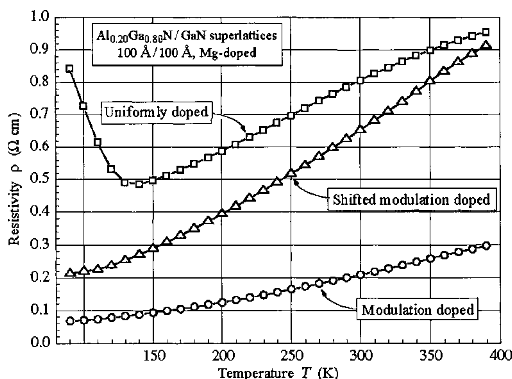

Fig. 2. Variable temperature resistivity data of a modulation-doped, a shifted-modulation-doped, and a uniformly doped $Al_{0.20}Ga_{0.80}N$/GaN superlattice

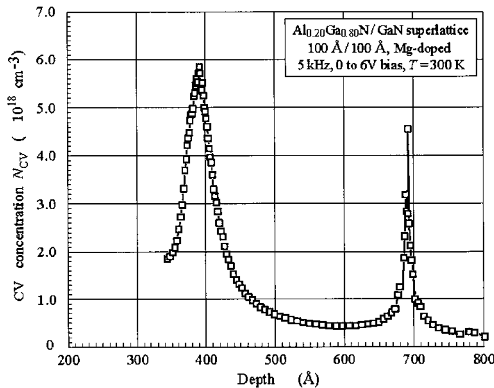

Fig. 3. $C-V$ concentration profile, N_{CV}, versus depth of shifted-modulation doped $Al_{0.20}Ga_{0.80}N$/GaN superlattice

cally with decreasing temperature, not exhibiting any freeze-out effect. This is due to the modulated valence band causing dopants to be ionized nearly independently of temperature. The improved resistivities demonstrated here should prove to be useful for the operation of GaN-based devices operating over a wide temperature range.

Capacitance–voltage measurements are presented in Fig. 3. The $C-V$ profile clearly shows the presence of a 2DHG with a peak at 390 Å and a FWHM of 41 Å. This corresponds to a 2D hole concentration of $\approx 4.9 \times 10^{13}$ cm^{-2}, in reasonable agreement with the 300 K Hall value of 6.7×10^{13} cm^{-2}.

The second peak at 690 Å shows the periodicity of the superlattice. The absolute position of the peaks is not as expected due to an uncertainty in material constants and a degradation of measurement phase angle. At positions greater than $\approx$800 Å, $C-V$ data cannot be obtained due to breakdown of the Hg probe Schottky contact.

Conclusion We demonstrate improved mobilities and resistivities in modulation- and shifted-modulation-doped $Al_{0.20}Ga_{0.80}N$/GaN superlattices versus a uniformly doped superlattice. The lowest 300 and 90 K resistivities we obtain, 0.21 and 0.068 Ωcm, respectively, are for the modulation-doped superlattice. The lowest 300 and 90 K mobilities we obtain are also for the modulation-doped superlattice: 8.9 and 36 cm^2/Vs, respectively. Self-consistent calculations for all SLs show the formation of 2DHGs at the SL interfaces nearest the Fermi level. The improved mobilities of the modulation-doped and shifted-modulation-doped superlattice compared to the uniformly doped superlattice are consistent with a reduction of neutral impurity scattering in the wells of the modulation-doped and shifted-modulation-doped samples. In addition, clear evidence of multiple 2DHGs is shown using $C-V$ profiling. The two-dimensional hole concentration of 4.9×10^{13} cm^{-2} calculated from $C-V$ data is in reasonable agreement with the 300 K Hall-effect value of the hole concentration.

References

[1] H. MARKOÇ and S. STRITE, J. Vac. Sci. Technol. B **10**, 1237 (1992).
[2] I. D. GOEPFERT, E. F. SCHUBERT, A. OSINSKY, and P. E. NORRIS, Electron. Lett. **35**, 1109 (1999).
[3] W. GÖTZ, N. M. JOHNSON, J. WALKER, D. P. BOUR, and R. A. STREET, Appl. Phys. Lett. **68**, 667 (1996).
[4] E. F. SCHUBERT, W. GRIESHABER, and I. D. GOEPFERT, Appl. Phys. Lett. **69**, 3737 (1996).
[5] P. KOZODOY, Y. P. SMORCHKOVA, M. HANSEN, H. XING, S. P. DENBAARS, U. K. MISHRA, A. W. SAXLER, R. PERRIN, and W. C. MITCHEL, Appl. Phys. Lett. **75**, 2444 (1999).
[6] A. SAXLER, W. C. MITCHEL, P. KUNG, and M. RAZEGHI, Appl. Phys. Lett. **74**, 2023 (1999).
[7] P. KOZODOY, M. HANSEN, S. DENBAARS, and U. K. MISHRA, Appl. Phys. Lett. **74**, 3681 (1999).
[8] F. BERNARDINI and V. FIORENTINI, Phys. Rev. B **57**, R9427 (1998).

[9] N. GRANDJEAN, B. DAMILANO, S. DALMASSO, M. LEROUX, M. LAÜGT, and J. MASSIES, J. Appl. Phys. **86**, 3714 (1999).
[10] M. LEROUX, N. GRANDJEAN, M. LAÜGT, J. MASSIES, B. GIL, P. LEFEBVRE, and P. BIGENWALD, Phys. Rev. B **58**, R13371 (1998).
[11] Freeware program "1D Poisson/Schrödinger", http://www.nd.edu/~gsnider/.
[12] W. GÖTZ, N. M. JOHNSON, J. WALKER, D. P. BOUR, H. AMANO, and I. AKASAKI, Appl. Phys. Lett. **67**, 2666 (1995).
[13] M. STUTZMANN, O. AMBACHER, A. CROS, M. S. BRANDT, and H. ANGERER, Mater. Sci. Eng. B **50**, 212 (1997)
[14] M. SHUR, B. GELMONT, and M. ASIF KHAN, J. Electron. Mater. **25**, 777 (1996).
[15] E. L. WALDRON, E. F. SCHUBERT, J. W. GRAFF, A. OSINSKY, M. J. MURPHY, and W. F. SCHAFF, Mater. Res. Soc. Conf. Proc. Vol. **639** (2000).